LINC

Learning about Interacting Networks in Climate

Marie Curie Initial Training Networks (ITN)

FP7- PEOPLE - 2011- ITN

Grant Agreement No. 289447

WorkPackage WP4: *Future Climate Change*

Deliverable D4.2

Report on the identification of climate shifts in the southern hemisphere

Marcelo Barreiro, Universidad de la República, Uruguay

Release date: 30 November 2013

Status: <*public*/*confidential*>

EXECUTIVE SUMMARY

One of the main objectives of the WP4 is to determine regime shifts in the evolution of the 20th century climate by analyzing reanalysis data and model simulations. From the atmospheric point of view, interannual climate variability can be divided into a contribution due to internal atmospheric dynamics and a forced influence from the oceans. This study has focused on characterizing changes in the oceanic influence over southeastern South America during the 20th century. To do so we have considered the oceanic regions that are known to influence precipitation over southeastern South America and constructed a network based on 4 indices that characterize the individual variability of ocean basins and rainfall. Results show that during southern hemisphere springtime the influence of the oceans has varied significantly over the last 100 years, presenting three periods of synchronization among oceans basins and rainfall. These synchronization periods are, in turn, different in the sense that the main interacting nodes during the 30's are the equatorial Pacific, the tropical north Atlantic and rainfall, while during the 70's and 90's the most important nodes are the equatorial Pacific, the Indian ocean Dipole and rainfall. A the same time, it is clear that El Niño dominates the forcing over southeastern South America. These results pose clear questions regarding why are there periods of synchronization, and why are they characterized by different roles of the ocean basins. We presented a first hypothesis related to the strength of the variability in each basin. Future work includes understanding the physical processes responsible for the interaction among nodes through analysis of simulations and study if these periods of synchronization may change their characteristics in a future scenario of climate change.

The following elements should be included:

1) The main objective addressed by the deliverable (with reference to the Description of Work [1])
2) Contribution of the deliverable to the goals of LINC, including its impact on other WPs and the target audience of the deliverable.
3) Summary of the deliverable, including main results and follow-up actions

Deliverable Identification Sheet

Grant Agreement No.	**PITN-GA-2011-289447**
Acronym	**LINC**
Full title	**Learning about Interacting Networks in Climate**
Project URL	http://climatelinc.eu/
EU Project Officer	Lucia PACILLO

Deliverable	**D4.2 Report on the identifical of climate shifts in the southern hemisphere**
Work package	**WP4 Future Climate Change**

Date of delivery	**Contractual**	M 24	**Actual**	30-Nov-2013
Status	version. 1.00		final ☑ draft ☐	
Nature	Prototype ☐ Report ☑ Dissemination ☐			
Dissemination Level	Public ☐ Consortium ☑			

Authors (Partner)	**Marcelo Barreiro, Universidad de la República; Ignacio Deza, Universidad Politecnica de Cataluña, Veronica Martin, Universidad de la Republica; Cristina Masoller, Universidad Politecnica de Cataluña**			
Responsible Author	Marcelo Barreiro		**Email**	barreiro@fisica.edu.uy
	Partner	Universidad de la República	**Phone**	

Abstract (for dissemination)	<summary description of document content>	
Keywords	<key word 1><key word 2>…	

Version Log			
Issue Date	**Rev No.**	**Author**	**Change(s)**
dd-mm-yy	001	<author>	<description of the changes made to preceding draft>

TABLE OF CONTENTS

Marie Curie Initial Training Networks (ITN) i
EXECUTIVE SUMMARY ..... **II**
Learning about Interacting Networks in Climate iii
TABLE OF CONTENTS ..... **IV**
1 INTRODUCTION **1**
2 DATA AND METHODOLOGY **2**
3 ANALYSIS OF RESULTS **5**
4 SUMMARY **13**
5 REFERENCES **13**
5.1.1 References 13
ANNEX I – SUPPORTING DOCUMENT 1 ..... **14**
ANNEX II – SUPPORTING CHART 2 ..... **14**

1 INTRODUCTION

Southeastern South America presents large rainfall variability from interannual to interdecadal time scales that has significant agricultural, environmental, energy and economic impacts. Several studies have shown that the tropical Pacific, Atlantic and Indian oceans influence rainfall variability in the subtropics through different mechanisms (e.g., Diaz AF., et al., (1998), Yulaeva and Wallace (1994), Grimm et al., (2000), Alexander et al., (2002), Saji et al., (2005), Taschetto and Wainer (2008), Chang et al., (2008), Barreiro et al., (2008)). Moreover, these oceans interact among them forcing sea surface temperatures in remote basins through atmospheric and oceanic teleconnections (e.g., Barreiro et al., (2008), Yoo et al., (2013), Chunzai et al., (2009), Dommenget et al., (2006), Jansen et al., (2009), Frauen et al., (2012), Rodriguez-Fonseca et al., (2009), Ding et al., (2012), Enfield et al., (1997), Saravanan et al., (2000) and Alexander et al., (2002)). However, it is not clear to date how the sea surface temperature anomalies in different basins interact to induce rainfall anomalies and neither how the interaction among the oceans and their influence on rainfall variability has evolved with time.

In this study we consider the interaction among oceans and their influence on subtropical South America rainfall from a complex network perspective, in order to know more about their collective behavior and their dynamic of interaction.

The complex networks theory has emerged as an important mathematical tool in the analysis of the complex systems, having been applied in many areas of the natural and social sciences. In particular, giving the complexity of the inter-relations among the different elements that constitute the environment and the huge economic and social impacts of climate variability and change for future generations, the complex networks theory is also well positioned to be useful tool in the analysis and study of global and regional climate. Recent studies have shown that this theory can indeed yield light into interesting and previously unknown features of our climate. Many of them construct a climate network considering as nodes all grid points of gridded data, and the links are inferred through some dependence measure such as cross correlation (Tsonis et al., (2007), Tsonis et al., (2008), Yamasaki et al., (2008), Swanson et al., (2009)), mutual information (Barreiro et al., (2011) and Donges et al., (2009)), phase synchronization analysis (Yamasaki et al., (2009)). Although less numerous, there are other studies in which the network's nodes are represented by different climate indices that characterize certain region of the Earth. For example, in the work of Tsonis et al., (2007) the network is defined considering as nodes the major modes of variability in the North Hemisphere, that is, the Pacific Decadal Oscillation (PDO), the North Atlantic Oscillation (NAO), the El Niño/Southern Oscillation (ENSO) and the North Pacific Oscillation (NPO). They investigated their collective behavior considering the mean distance of cross correlation as the synchronization measure and defined synchronization as those periods when the network's nodes were interacting such that the distance reached a statistically significant threshold. They found that the network synchronized several times in the period 1900-2000, and when the synchronous state was followed by a steady increase in the coupling strength between climates indices the synchronous state was destroyed and a new climate stage emerged.

In this work, we construct a network following the Tsonis scheme (Tsonis, et al., (2007)), and study the collective behavior of the network's nodes and their evolution over the 20th century. The network is defined with an index that characterizes precipitation over Southeastern South America (particularly over Uruguay) and different indices that characterize the regions of the tropical oceans, that are known to influence the subtropical South America rainfall: El Niño/Southern Oscillation (Niño3.4), the Tropical North Atlantic (TNA), and the Indian Ocean Dipole (IOD). These four climate indices will make up the nodes of the climate network. Here we investigate the collective behavior of the network focusing on detection of synchronization events in order to know more about the dynamics that characterize their interaction and how the 'collective-behavior' has evolved with time. The synchronization events will be defined considering the mean distance of cross – correlation.

2 DATA AND METHODOLOGY

2.1. Data

With the purpose of defining the different tropical oceanic indices mentioned above, in this work we consider the monthly mean Sea Surface Temperatures (SST) reanalysis data from 1901 to 2006 from ERSSTv3b (Extended Reconstructed Sea Surface Temperature, available on web page: http://iridl.ldeo.columbia.edu/SOURCES/.NOAA/.NCDC/.ERSST/.version3b/.sst/), and from HadSST (Hadley Center Sea Surface Temperatures, available on web page: http://www.metoffice.gov.uk/hadobs/hadsst3/data/download.html). The Precipitation index is defined considering the monthly mean observed data from the Global Precipitation Climatology Center (GPCCv5, available on web page: http://www.esrl.noaa.gov/psd/data/gridded/data.gpcc.html). We compare the obtained networks (from ERSSTv3b and from HadSST) to test their robustness.

We also consider the simulated precipitation from an AGCM forced with observed Sea Surface Temperatures (SST) to help understand us the network variations. We use the ICTP-AGCM and construct an ensemble of 9 runs initializing the model with different atmosphere conditions, but all having the same SST boundary conditions. The precipitation index is considered as the ensemble mean precipitation over the region of interest, and thus by construction it will mainly represent the oceanically-forced rainfall variability. The ICTP-AGCM is forced with observed SST from the ERSSTv2 dataset. Sea Surface Temperatures indices in the case of the model output are very similar to those constructed from ERSSTv3b and HadSST datasets. Thus, the main difference in the networks constructed from observed and model data arise due to differences in the evolution of precipitation.

2.2. Methodology

The methodology consists of several steps:

First, we define the climate indices by latitudinal and longitudinally averaging of the sea surface temperatures and precipitation in the different regions that represent each index. The latitudinal and longitudinal average is carried out considering the regions that appear reflected in the table 1. In the case of the

Indian Ocean Dipole we subtract the average between the two boxes to construct the index. We also eliminate the trend of the time series and compute the monthly anomalies removing the climatological cycle from 1901 to 2006. The indices are normalized.

Second, we will consider individual trimesters to construct the networks. Thus before taking 3-month mean and in order to avoid aliasing affects of high frequency, we first apply a low-pass Lanczos filter with cutoff frequency of 1/12 to the monthly mean time series.

Third: following the Tsonis' scheme (Tsonis et al, (2007)), we construct the network considering the mean network distance definition as synchronization measure. Mathematically, the mean network distance can be defined as following:

$$d(t) = \frac{2}{N(N-1)} \sum_{i,j} \sqrt{2(1-|\rho_{ij}^{t}|)}$$

where t denotes the time in the middle of a sliding window of width (Δt=11 years), N represents the number of network's nodes (in this case, 4) and ρ_{ij}^{t} is the cross correlation coefficient between nodes i and j in the interval [$t-\frac{\Delta t}{2}$, $t+\frac{\Delta t}{2}$]. This measure is useful to study and describe the variations in the network's topology. The distance can be thought as the average correlation between all possible network's nodes and is interpreted as a measure of the synchronization of the network's components. Synchronization between nonlinear (chaotic) oscillators occurs when their corresponding signals converge to a common, albeit irregular, signal. Note that a distance of zero corresponds to a complete synchronization and a distance of $\sqrt{2}$ characterizes a set of uncorrelated nodes. In turn, the above mathematical expression uses the absolute value of cross correlation because we are interested in knowing when the interactions between two nodes are significant independently of the sign.

The correlations coefficients (and therefore the mean network distance for each year) are computed based on seasonal means of the monthly anomaly values of the indices from September to November for the case of Niño3.4 index, and from November to December for the remainder indices (TNA, IOD and precipitation). Therefore, our network's nodes are characterized by time series of 106 values, each one representing the seasonal mean anomalies of three months of each year (SON for El Niño3.4 and OND for the rest).

Fourth, to determine the spectral characteristics of the time series we compute the lag-1 autocorrelation coefficient. Only for the case of Niño3.4 this correlation value is significant. Thus, we calculate the 95% significance level of correlation values generating 1000 surrogates time series of each index under the following null hypothesis: the IOD, TNA and precipitation indices represent a sample from a population of white noise and the El Niño3.4 is behaved as a red noise (represented by an first order autorregressive process, AR-1). For each member of that population (that is, for each surrogate time series of each index) we compute the network distance time series considering a sliding window of 11-years length. In this way, we will have 1000 surrogate time series of the

mean network distance, which allows determining the 5% level. Finally, we consider that there is a statistically significant synchronization event when the mean network distance is bellow this threshold.

This procedure is carried out for the two observed SST datasets and for the ICTP-AGCM's output. We employ two different observed SST dataset in order to test the sensitivity of synchonizations events to the employed dataset. Moreover, if the network constructed with simulated rainfall can reproduce the observed synchronization events and the rainfall plays an important role in the synchronization, model's output will allows us to study the global circulation anomalies that connect the different oceans on the region of interest. In the next section, we analyze the network topology.

Index short name	Long name index	Earth's region	
		Latitude range	Longitude range
NINO3.4	El Niño3.4	5ºN-5ºS	170ºW-120ºW
TNA	Tropical North Atlantic	10ºN-30ºN	60ºW-30ºW
IOD	Indian Ocean Dipole	10ºS-10ºN 10ºS-0ºN	50ºE-70ºE 90ºE-110ºE
PCP	Precipitation Southeastern South America (particularly over Uruguay)	40ºS-25ºS	60ºW-50ºW

Table 1: Geographical regions of each index that make up our network's nodes. The indices are defined considering the longitudinal and latitudinal average of the sea surface temperatures and precipitations in the specified regions in this table. In the Indian Ocean Dipole case, the index is computed from the difference between the 2-D average Sea Surface Temperature in the west region and the 2-D average in the east region. These regions appear plotted in the Figure 2.1.

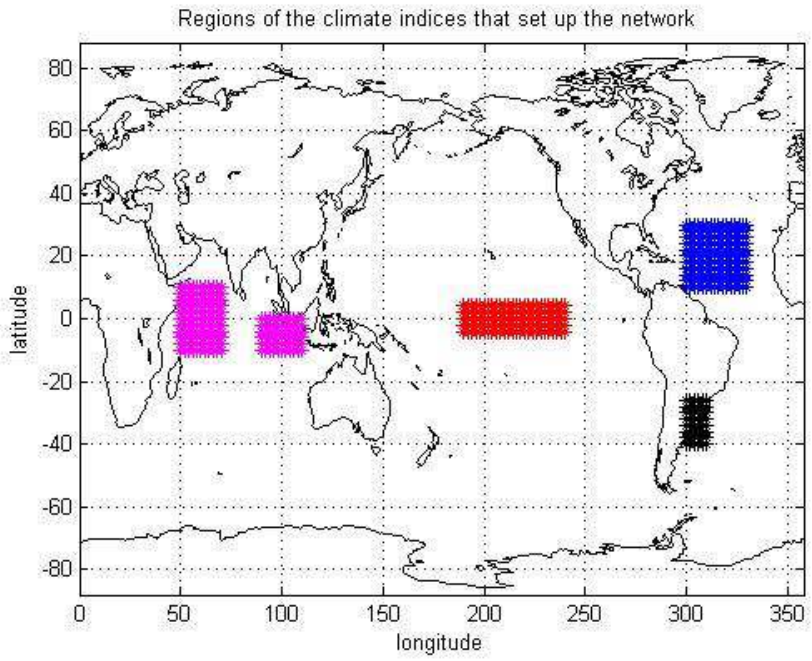

Figure 2.1. Regions that represents the climate indices: Indian Ocean Dipole (IOD) in magenta, Niño3.4 in red, the Tropical North Atlantic (TNA) in blue and the precipitation over Southeaster South America in black.

3 ANALYSIS OF RESULTS

In this section we describe the general features of the network, analyze its topology and study the physical mechanisms evolved.

3.1 Generals features of the network distance time series

The network distance time series is computed with Niño3.4 index centered on austral spring season (SON) and the rest of the indices on October-November-December (there is one month lag between Niño3.4 and the others network's nodes). Figure 3.1 represents this time serie. The red, blue and green lines represent the network distance computed from ERSSTv3b, HadSST and ICTP-AGCM's output, respectively and the horizontal dot black line represents the threshold level.

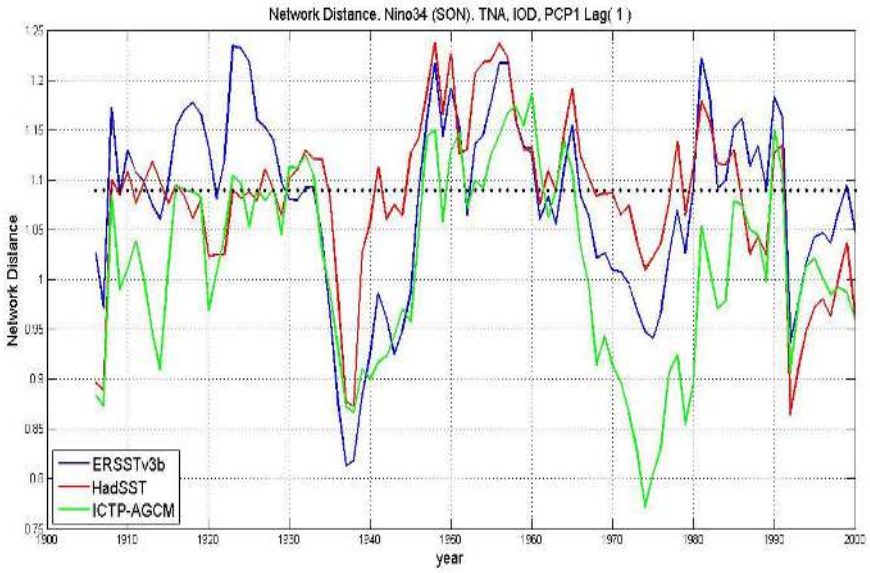

Figure 3.1. Network distance time series from 1901 to 2006. Red, blue and green lines represent the mean distance computed from ERSSTv3b, HadSST and ICTP-AGCM's output respectively. The horizontal black dot - line represents the threshold level. For each time step, the network distance is calculated considering the definition given by Tsonis et al., (2007) and a sliding window of 11 years length.

The major features can be summarized as follows:

1. As can be seen in this figure, the network distance is characterized by an interannual and interdecadal variability, having three periods in which both the observed (ERSSTv3b and HadSST) and simulated (ICTP-AGCM) networks distances presents synchronization (the network distance time series is under the threshold level). The first period is developed from 1933 to 1945, the second period covers 1966-1978 and the last one 1991-2000.
2. The fact that the two observed time series evolve in a way more o less similar in most of the period of study guarantees that the synchronizations events are not consequence of the employed dataset. It must be noted that during the first thirty years, the two observed datasets do not evolve in a similar way and this could be due to the scarcity of the observed data.
3. In turn, we can see that there are periods in which the magnitude of the simulated network distance evolution agrees well with the observations (1933-1945, and 1991-2000) and an others in which this is not the case (the period developed from 1966 to 1978). This suggests the following question: Why are there synchronization periods in which the magnitude of the observed and simulated network distances evolve similarly and others in which does not?

   To answer this question we have to take into account that the precipitation are made up by two sources of variability: internal or intrinsic variability and ocean forced variability:

$$PCP = PCP_{internal} + PCP_{ocean} + PCP_{forced}$$

¿¿¿¡¿¿

The simulated network distance is computed considering the observed ERSSTv2 Sea Surface Temperatures from the ICTP-AGCM, and the precipitation from the ensemble mean of 9 experiments with different initial conditions. Therefore, differences between the network distance calculated with observations and simulation should arise mainly due to the precipitation index.

Thus, let's consider as a starting point the possibility that the rainfall index is not important in the networks, that is, the correlation coefficients between the ocean indices and precipitation are close to zero, and then the oceans do not influence rainfall variability over Southeastern South America. In this case the similarity between observed and simulated networks is obvious given that both use observed SSTs. To check if this is the case it is necessary to know which is the relative precipitation weight (RPW) in the network (that is, what is the importance of the precipitation in our network? or in other words, Is the precipitation index a disconnected network's node?). This parameter is computed considering the following mathematical expression:

$$RPW = \frac{\frac{\sqrt{2}}{2} - d_{op}}{\frac{\sqrt{2}}{2} - d}$$

where d_{op} represents the network distance calculated considering only the correlation coefficients between the precipitation index and the ocean indices (that is, the interaction between oceans is not taken into account). The max and minimum values of the RPW are one and zero respectively, in such a way that the higher values of the RPW are associated with a higher importance (or weight) of the precipitation index in the network. In other words, the higher values of the RPW imply the longer influence of the tropical oceans on rainfall.

The relative precipitation weight is plotted in Figure 3.2. (blue line). It shows that in the first (1933-1945) and third (1991-1978) synchronization periods the relative precipitation weight presents two relative maxing, indicating that the role of the rainfall index in the network is important. Thus, in the first and third periods of synchronization the precipitation index is important in the network and the magnitude of the network distance simulated by the model follows the observed ones. Therefore, it is likely the oceanically forced signal on rainfall is strong and the ensemble mean precipitation represents it correctly.

To further substantiate this we computed the network distance for each of the 9 ensemble members of the experiment and defined a confidence interval given by the max and minimum values for each 11 years window (Figure 3.3). Overall, it is clear the observed network distance falls within the confidence interval, independent on the RPW, suggesting that the simulated rainfall is close to the observed one. The figure also shows that in the three

synchronizations periods the magnitude of the simulated distance is just outside the confidence interval suggesting large rainfall variability within the ensemble that is filtered out in the average procedure. Moreover, for the first and third synchronization periods the observed distance is close to the lower end of the confidence interval suggesting a strong oceanically – forced signal (because the magnitude is close to that of the ensemble mean). On the other hand, as the second synchronization period the observed network distance is well within the confidence interval, suggesting a weak oceanically forced signal embedded in large internal atmospheric variability.

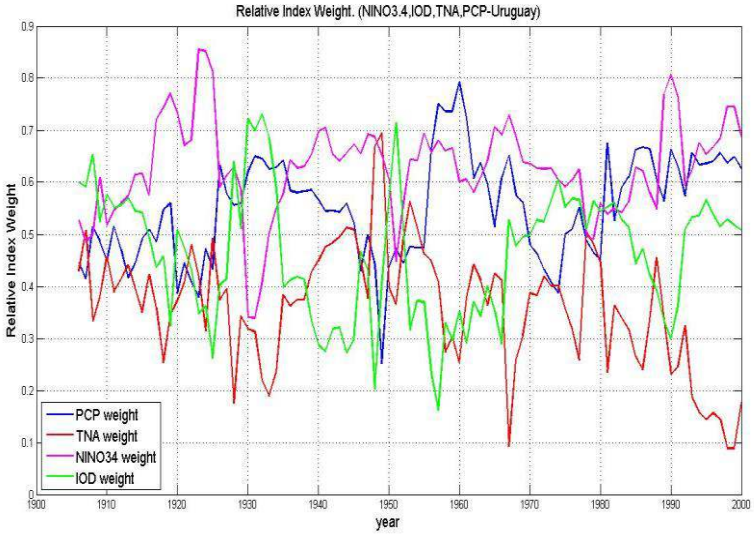

Figure 3.2. Relative Weight Index time series. This parameter indicates us what is the importance of the each node in the network and is enclosed between zero and one. Higher values of the relative weight are associated with higher importance of the particularly index in the network.

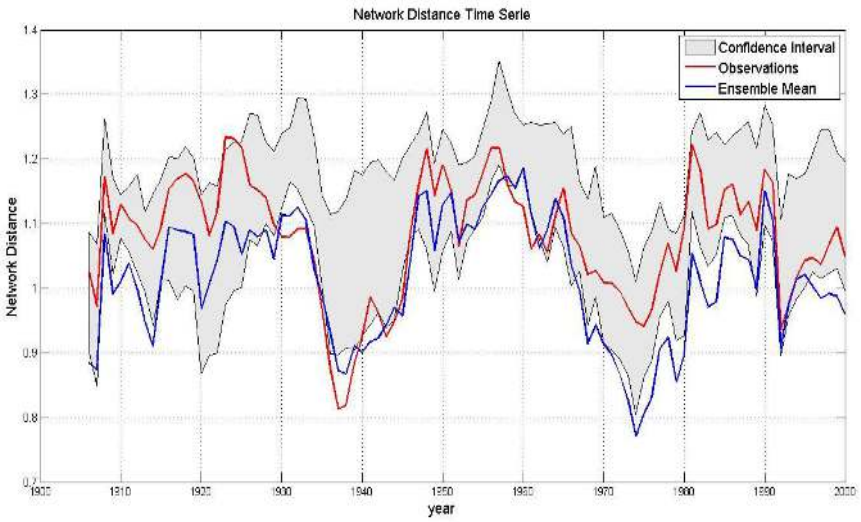

Figure 3.3. Simulated confidence interval for the network distance time series from 1901 to 2006. The blue and red lines represent the ensemble mean and observed network distance time series respectively.

3.2 Network's topology

The major aim of this section is to determine the structure of the network in each synchronization period and which nodes are connected. To address this issue, the correlation coefficient time series between each pair of network's nodes are computed (Figure 3.4). The horizontal brown broken lines represent the thresholds at 95% and 90% significance levels considering a two tails t-test. We consider that two nodes are strongly connected if the cross correlation coefficient is over the 95% significance level, and that they are weakly connected when it lies between the 90% and 95% significance levels. It follows that there are two types of networks characterized with different connections among nodes. That is, while in the first synchronization period the connected nodes are NINO3.4 with PCP, TNA with PCP and NINO3.4 with TNA; in the second and third periods they are NINO3.4 with PCP, IOD with PCP and NINO3.4 with IOD (Figure 3.6 represents a scheme of this result). This result is also evident if we look at the correlations maps (Figure 3.5) between the precipitation index and the Sea Surface Temperatures anomalies.

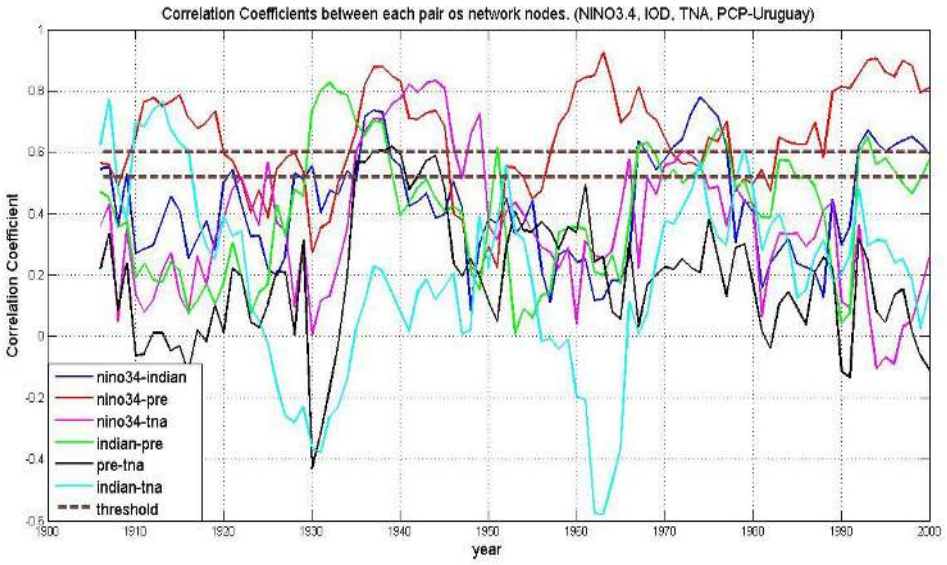

Figure 3.4. Cross correlation coefficient between each pair of network's nodes. The horizontal brown broken lines represent the thresholds levels at 95% and 90% significant level.

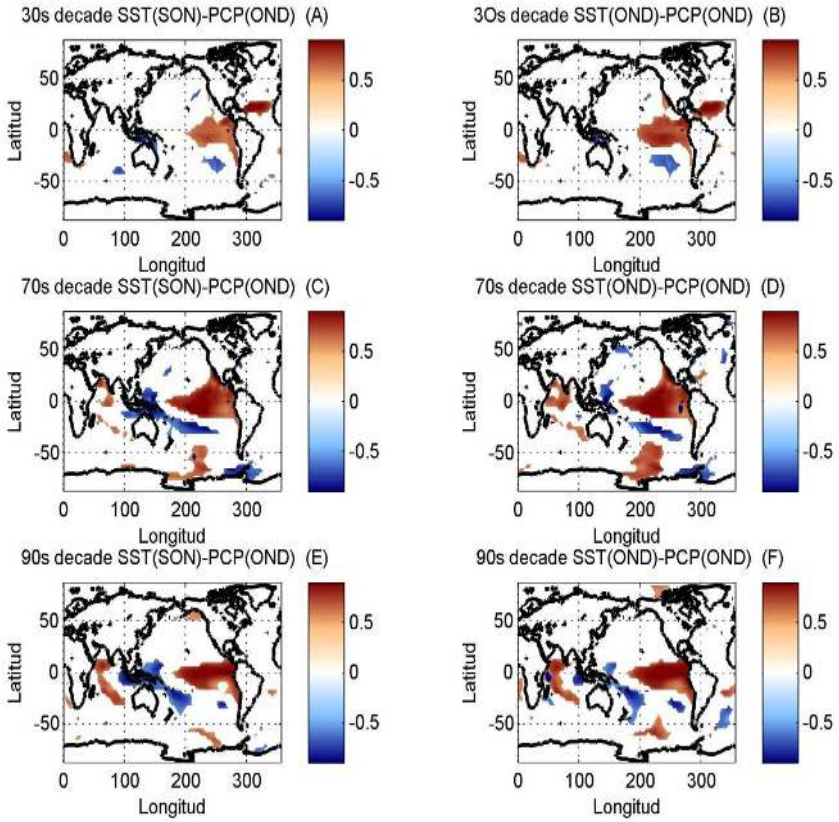

Figure 3.5. Correlation maps between precipitation index over Southeastern South America centered on OND and anomalies sea surface temperatures. The temperatures are centered on SON (left panel) and on OND (right panel). Maps computed considering ICTP-AGCM output.

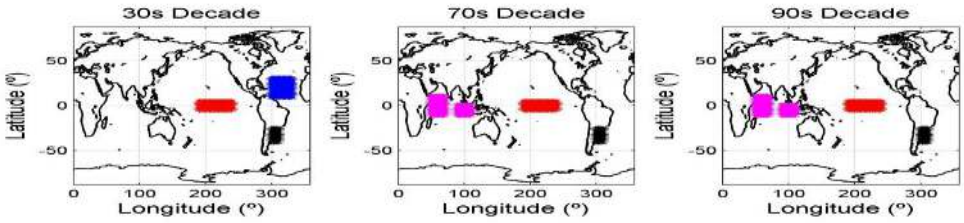

Figure 3.6. Regions of the world that has an important role in the rainfall variability over Southeastern South America. These regions represent the nodes of the network which are interacting among them in each period of study.

These results suggest the following question: Why in the last two synchronization events the IOD has an important role in the networks and in the first period it does not? And, why does the TNA appear like an interactive network's node in the first period and not in the other two? To help addressing

this question we calculated the standard desviation of each ocean index considering sliding windows of 11 years length (Figure 3.7, upper for the Niño3.4, middle for TNA, and bottom for the IOD). The standard desviation time series of the Niño3.4 index during the periods 1966 to 1978 and 1991 to 2000 (second and third synchronization events) is larger than during the first half of the 20th century (when the first synchronization event is found). This indicates that the El Niño events of the second half of the 20th century were more intense than in the first half. We hypothesize that the intensification of this equatorial Pacific phenomena allowed that the El Niño forced signal was felt by Indian Ocean, and this basin answered with a warming in the western section (see regression map of El Niño and SST in the second synchronization period, Figure 3.10 (A)) or with the generation of a dipole zonal mode (see regression map of El Niño and SST in the third synchronization period, Figure 3.11 (A)). These two types of responses of the Indian Ocean to the El Niño forcing can be also observed in the standard desviation time serie of the IOD index (Figure 3.7 bottom panel). In the second and third synchronization periods (developed from 1966 to 1978, and from 1991 to 2000) we can see that the standard desviation is longer in the third period than in the second, consistent with a stronger dipole in the third period. In turn, in the period from 1933 to 1945 (first synchronization event) the IOD signal is weaker than in the other two periods of study.

On the other hand, if we look at the standard desviation time series of TNA, it is seen that the period of maximum value coincides with the first synchronization period in which this index is an interactive node of the network. Moreover, this period coincides with the maximum cross correlation coefficient between the TNA and El Niño3.4 indices. Now then, taking into account that the precipitation, the IOD and TNA are forced by El Niño, it could be that the links between IOD - Precipitation, and TNA-Precipitation appear in the networks as consequence of having a common forcing: El Niño. Generally then we could ask which links of the networks are direct and which are indirect? To address thus question we compute the partial correlation maps between precipitation index and the SST field considering El Niño3.4 index constant (Figure 3.8). In that figure we can see that considering the Niño3.4 index constant the links between IOD and precipitation in both second and third synchronization events disappear not being so in the case of the TNA. This suggests that while the link between the IOD and precipitation is indirect, the link between TNA and precipitation is direct. This also suggests that SST anomalies in TNA are not only forced by El Niño.

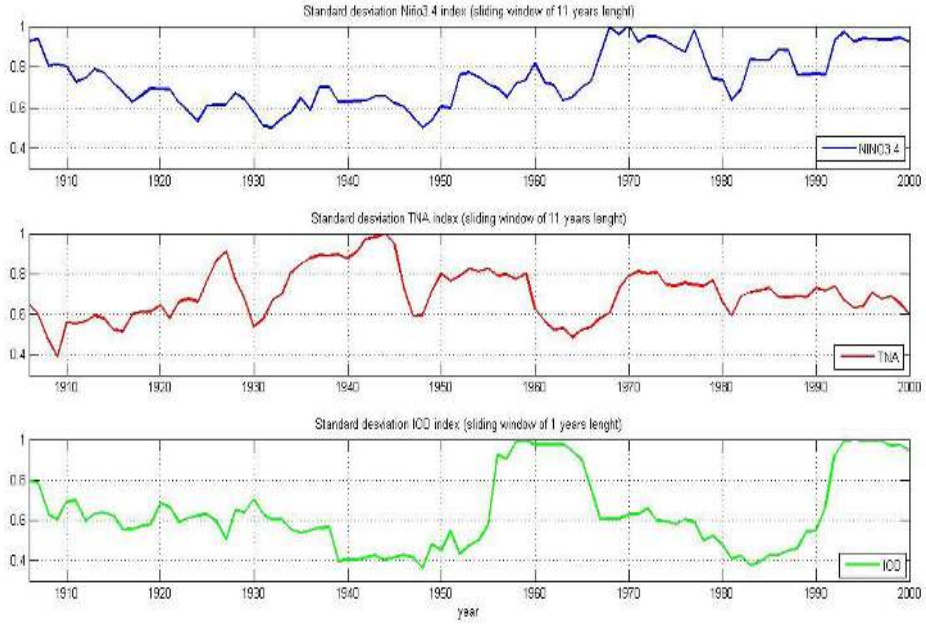

Figure 3.7. Standard desviation of the Niño3.4 (upper), TNA (middle) and IOD (bottom) index.

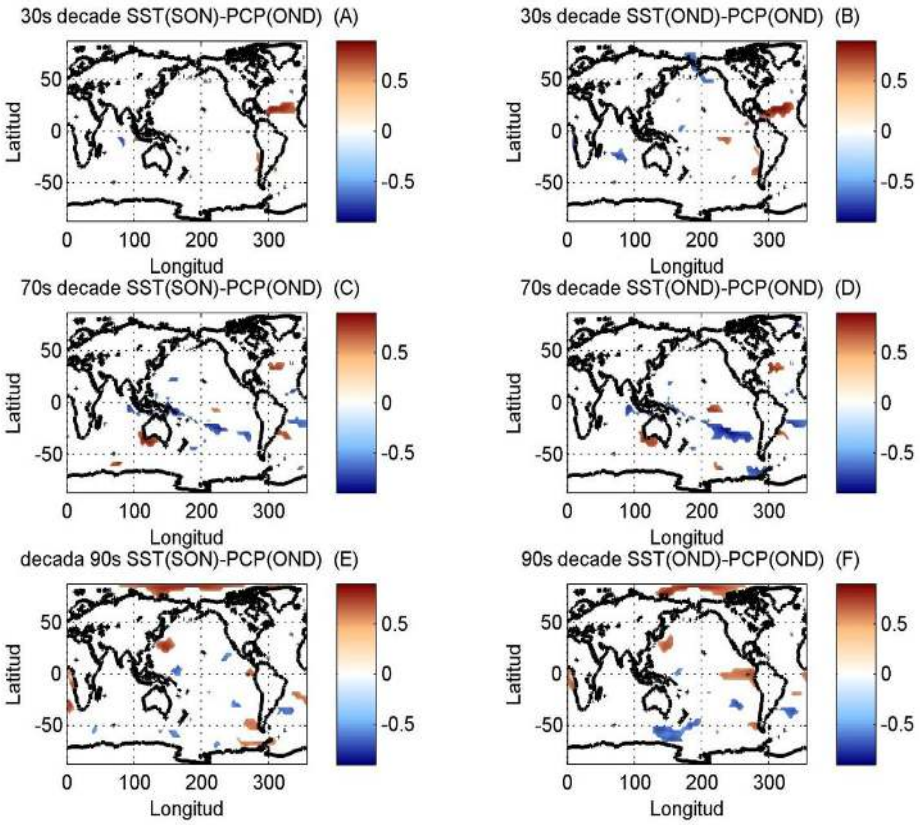

Figure 3.8. Partial cross correlation map between the precipitation index and the sea surface temperature field considering El Niño3.4 index constant. Upper panels from 30's decade, middle panels from 1966 to 1978 and bottom panels from 90's decade. Maps computed considering ICTP-AGCM output.

4 SUMMARY

One of the main objectives of the WP4 is to determine regime shifts in the evolution of the 20th century climate by analyzing reanalysis data and model simulations. From the atmospheric point of view, interannual climate variability can be divided into a contribution due to internal atmospheric dynamics and a forced influence from the oceans. This study has focused on characterizing changes in the oceanic influence over southeastern South America during the 20th century. To do so we have considered the oceanic regions that are known to influence precipitation over southeastern South America and constructed a network based on 4 indices that characterize the individual variability of ocean basins and rainfall. Results show that during southern hemisphere springtime the influence of the oceans has varied significantly over the last 100 years, presenting three periods of synchronization among oceans basins and rainfall. These synchronization periods are, in turn, different in the sense that the main interacting nodes during the 30's are equatorial Pacific, the tropical north Atlantic and rainfall, while during the 70's and 90's the most important nodes are the equatorial Pacific, the Indian ocean Dipole and rainfall. A the same time, it is clear that El Niño dominates the forcing over southeastern South America. These results pose clear questions regarding why are there periods of synchronization, and why are they characterized by different roles of the ocean basins. We presented a first hypothesis related to the strength of the variability in each basin. Future work includes understanding the physical processes responsible for the interaction among nodes through analysis of simulations and study if these periods of synchronization may change their characteristics in a future scenario of climate change.

5 REFERENCES

[1] LINC Grant Agreement no. LINC-289447, Annex I (‘Description of Work’), 1 Dec 2011.

[2] Alpha A., Beta B., Gammow C., *I Blame Place Illusion and Plausibility for the Mishap with the Chainsaw*, Presence: Teleoperators and Virtual Environments, special issue, 2010. Doi: 10.1016/j.bspc.2009.09.004.

5.1.1 References

Please ensure that your references are denoted in the text as cross links, e.g. [1] or [2].

Where possible, make sure that you include the doi reference of a publication. The Digital Object Identifier (DOI®) System is for identifying content objects in the digital environment. DOI® names are assigned to any entity for use on digital networks. They are used to provide current information, including where they (or information about them) can be found on the Internet. Information about a digital object may change over time, including where to find it, but its DOI name will not change.

For further information see www.doi.org.

ANNEX I – SUPPORTING DOCUMENT 1

<doc>

ANNEX II – SUPPORTING CHART 2

<chart>